

HLA: Hadamard Linear Attention

Hanno Ackermann Hong Cai Mohsen Ghafoorian Amirhossein Habibian

Qualcomm AI Research¹

Abstract

The attention mechanism is an important reason for the success of transformers. It relies on computing pairwise relations between tokens. To reduce the high computational cost of standard quadratic attention, linear attention has been proposed as an efficient approximation. It employs kernel functions that are applied independently to the inputs before the pairwise similarities are calculated. That allows for an efficient computational procedure which, however, amounts to a low-degree rational function approximating softmax.

We propose Hadamard Linear Attention (HLA). Unlike previous works on linear attention, the nonlinearity in HLA is not applied separately to queries and keys, but, analogously to standard softmax attention, after the pairwise similarities have been computed. It will be shown that the proposed nonlinearity amounts to a higher-degree rational function to approximate softmax. An efficient computation scheme for the proposed method is derived that is similar to that of standard linear attention. In contrast to other approaches, no time-consuming tensor reshaping is necessary to apply the proposed algorithm. The effectiveness of the approach is demonstrated by applying it to a large diffusion transformer model for video generation, an application that involves very large amounts of tokens.

1. Introduction

The transformer architecture has demonstrated remarkable success across a wide range of domains, for instance, question answering (Sima et al., 2024), reasoning (Wei et al., 2022), and even tasks such as 3D reconstruction (Wang et al., 2024). An important reason for this success is the

attention mechanism which facilitates information exchange between the elements of an input sequence or set. An important limitation of the standard attention mechanism is its quadratic complexity with respect to the length of the input sequence. Although recent advances (Dao et al., 2022; Dao, 2023; Shah et al., 2024) have mitigated the quadratic memory complexity, the computational complexity remains quadratic. Linear attention mechanisms have been proposed as scalable alternatives. However, despite their improved efficiency, linear attention-based transformers (Katharopoulos et al., 2020; Schlag et al., 2021) exhibit reduced performance compared to those that use standard attention.

Attention scores due to softmax attention typically have very few large values, whereas the majority of its outputs are tiny. It has been confirmed that these matrices have very high ranks (Zhang et al., 2025). Most works on linear attention focus on approximating softmax by separable kernels. This causes a low-rank constraint which prevents linear attention to precisely approximate the output of softmax attention (Fan et al., 2025a). As pointed out by (Letourneau et al., 2024), this constraint amounts to a low-degree rational function. It has been proposed to augment the linear attention model with extra terms to mitigate the low-rank constraint (Fan et al., 2025a), yet this reduces the efficiency of linear attention. A different approach for enhancing the performance of linear attention is gated delta networks (Schlag et al., 2021; Yang et al., 2025a). This algorithm attempts to suppress less relevant token interactions by decay functions, thereby prioritizing more informative dependencies within the input sequence. Recently, hybrid attention mechanisms have been proposed to address this issue by combining both softmax-based quadratic attention and linear attention (Zhang et al., 2025). Although this is a promising approach, it in fact still has quadratic complexity.

In standard linear attention models, nonlinear transformations, ie the separable kernels, are applied *prior* to computing pairwise interactions, resulting in a low-rank approximation of the full attention matrix. This contrasts with softmax-based attention, where the nonlinearity is applied *after* the pairwise interactions have been computed. In this work, we introduce a novel nonlinearity for linear attention, ie, Hadamard Linear Attention (HLA). Unlike existing approaches, the proposed nonlinearity can also be applied

¹Qualcomm AI Research is an initiative of Qualcomm Technologies, Inc.. Correspondence to: Hanno Ackermann <hackerman@qualcomm.com>.

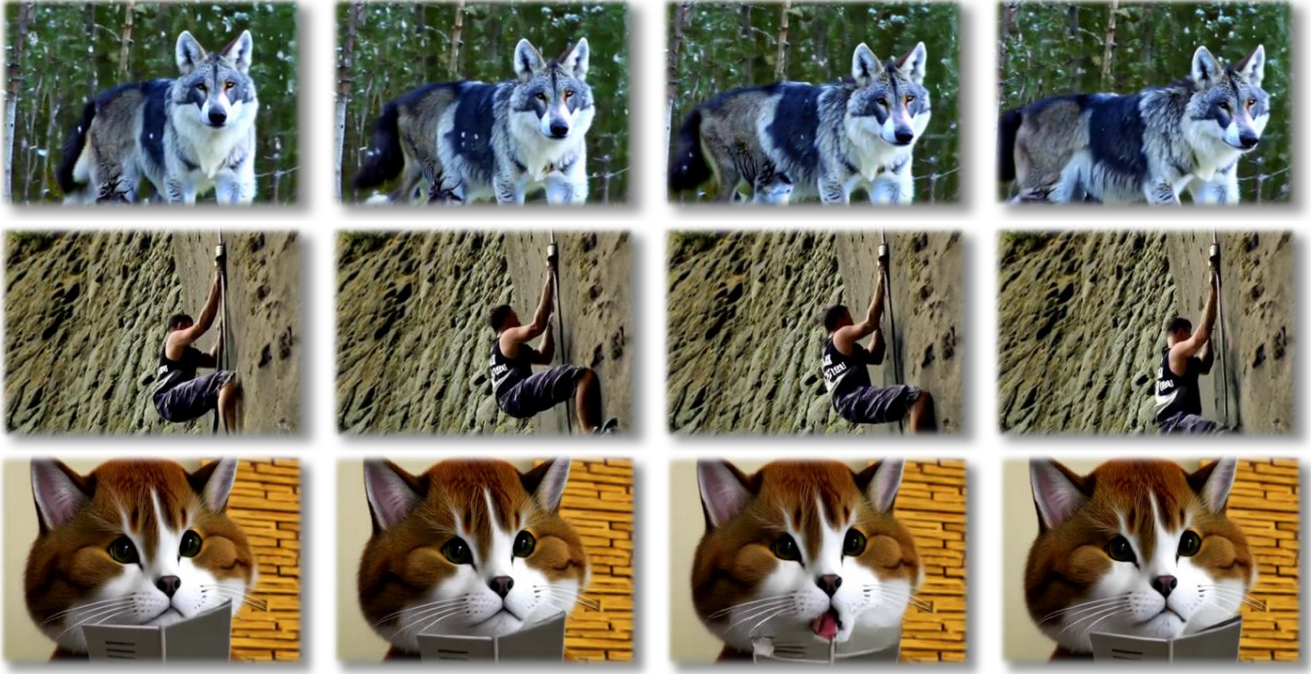


Figure 1. Results generated using the proposed video diffusion transformer (**HLA-3F-R1-10**, see sec. 5.1 for more details) using Hadamard Linear Attention.

after the pairwise interactions have been computed, thereby aligning more closely with the behavior of standard softmax attention. We derive an efficient computation scheme for the proposed attention mechanism, preserving the scalability benefits of linear attention.

An important advantage of the proposed algorithm is that it can be directly applied to the sequence, unlike other algorithms (Zhang et al., 2025; Letourneau et al., 2024) which first require the reshape the tensor. While this reshaping operation is not measured by metrics such as the number of floating point operations (FLOPs), it may cause a higher latency especially on memory-constrained platforms¹. Furthermore, Hadamard Linear Attention considers the entire sequence through its attention mechanism whereas (Letourneau et al., 2024) only has a limited view via its receptive field.

Lastly, we propose a modification of gated attention: This method has been proposed to re-weight the outputs of the attention by a gating function that uses a sigmoid-normalized function of the inputs (Qiu et al., 2025). The authors report that this enhances performance and mitigates attention sinks. We could not confirm performance improvements in our ap-

¹When programming, we may stumble over this problem when we experience the error message *cannot backpropagate through non-contiguous tensor*. Which operations require a contiguously arranged tensor depends on the capabilities of the specific hardware.

plications, but propose a simplified variant of this technique that yields performance improvements.

This summarizes our contributions:

- We propose a novel algorithm for linear attention, Hadamard Linear Attention (HLA), which applies a nonlinear transform *after* pair-wise similarities have been computed.
- The higher polynomial degree of HLA compared to linear attention makes the model more expressive and allows for better results.
- The procedure is based on standard, hardware-friendly operations like `einsum`. It neither requires expensive operations like softmax nor dynamic indexing.
- On the challenging task of video generation which involves extremely long sequence lengths, our method shows on-par performance when comparing to state-of-the-art video diffusion models that use standard attention, while using up to 90% less compute.
- The results demonstrate that the novel attention mechanism can generate high-quality videos with significant dynamics without techniques such as windowing or the delta rule.
- Moreover, our model only requires 8 H100s to train.

2. Related Works

Linear attention has been proposed to solve the quadratic memory requirement and computation complexity that standard softmax-based attention has (Shen et al., 2024; Katharopoulos et al., 2020). It has been noted that algorithms relying on linear attention often perform poorly compared to algorithms using standard attention. The authors of (Schlag et al., 2021) point out that linear attention is equivalent to fast weight programmers (Schmidhuber, 1992). The same authors also propose to use a decay factor to hinder retention of irrelevant information over a sequence via the Delta rule. Since the latency of this algorithm increases with the sequence length, a chunked version of this algorithm has been proposed in (Qiu et al., 2025). For LLM training, a similar idea has been proposed in (Sun et al., 2023).

(Peng et al., 2021a; Choromanski et al., 2022; Qin et al., 2022; Meng et al., 2025) propose how to better approximate the exponential function in the context of linear attention. The low-rank constraint inherent to linear attention is a likely cause of the poor performance of linear attention. A solution has been proposed in (Fan et al., 2025a). Other approaches have been proposed as well, for instance based on maximal coding rate reduction (Wu et al., 2024) or locality sensitive hashing (Han et al., 2023).

A different approach to reducing the quadratic complexity of standard attention is State Space Methods (SSMs). They model the temporal change by a set of first-order differential equations which are recurrently applied to the input sequence. They can perform well on long-range tasks (Gu et al., 2022) and can match or even transformers in some tasks (Gu & Dao, 2024). Connections between linear attention and SSMs were revealed in (Dao & Gu, 2024). Using the delta rule as in (Schlag et al., 2021) can also benefit SSMs (Yang et al., 2025a). Drawing on ideas from SSMs, the authors of (Egorov et al., 2025) improve a standard attention mechanism without sacrificing performance.

Linear attention has been used to improve diffusion networks, for instance in (Xie et al., 2024; Zhu et al., 2024) for images. Linear attention improved by the delta rule has also been used in diffusion algorithms for video generation (Chen et al., 2025; Team et al., 2025). The authors of (Ye et al., 2025) improve standard attention by performing it twice and subtracting the two results.

Recently, (Zhang et al., 2025) and (Ghafoorian et al., 2025) combined softmax attention with linear attention for video diffusion. This idea is to model large values in the attention matrix by softmax, yet smaller ones by linear attention. While these hybrid methods offer good performance, they require dynamical indexing² and are not softmax-free

²Directly selecting one or multiple individual values in a tensor is not supported by some low-power compute units.

3. Attention

3.1. Softmax Attention

Let there be N tokens $\mathbf{X} = [\mathbf{x}_0^\top, \dots, \mathbf{x}_N^\top] \in \mathbb{R}^{N \times d}$ where the scalar d indicates the number of elements each of the vectors \mathbf{x}_i has. These input tokens are mapped to queries Q , keys K and values V by right-multiplying with learnable matrices W_q, W_k, W_v . The attention scores are the product QK^\top normalized by *softmax*. The attention mechanism used in (Vaswani et al., 2017) uses them to compute a convex combination of the values

$$\text{softmax} \left(\frac{1}{\sqrt{d}} QK^\top \right) V. \quad (1)$$

This explanation defines self-attention that compares the tokens \mathbf{x}_i and \mathbf{x}_j from the same sequence. The so-called cross-attention uses two different input sequences of tokens.

3.2. Linear Attention

The standard attention mechanism has been used with great success in many works, yet its compute and memory complexity are quadratic with respect to the calculation of the attention scores. Although a solution to quadratic memory complexity has been proposed by (Dao et al., 2022; Dao, 2023), these algorithms still require $\mathcal{O}(N^2)$ compute operations.

Linear attention has been proposed (Schlag et al., 2021; Katharopoulos et al., 2020; Schlag et al., 2021) as a solution to both problems. Its idea is to approximate the exp function using a separable kernel

$$\exp \langle \mathbf{x}_i, \mathbf{x}_j \rangle \approx K(\mathbf{x}_i, \mathbf{x}_j) = \langle \phi(\mathbf{x}_i), \phi(\mathbf{x}_j) \rangle. \quad (2)$$

Due to the separability of the kernels, the order of matrix multiplication is changed for linear attention

$$\phi(Q) (\phi(K)^\top \cdot V) = \phi(Q) \cdot C \quad (3)$$

which avoids explicitly computing the attention scores whereby the complexity is reduced to $\mathcal{O}(N)$ since $\phi(K)^\top \cdot V$ forms the $d \times d$ *context* matrix. Matrix C in equation 3 is often called the context. (Fan et al., 2025b) highlights that the performance of linear attention mechanisms may degrade due to mapping queries in a d -dimensional space by equation 3 instead of the more expressive mapping in an N -dimensional space by equation 1 due to

$$\text{rank}(\phi(Q) \cdot C) \leq \min(\text{rank}(\phi(Q)), \text{rank}(C)) \quad (4)$$

Random Fourier Features have been proposed by (Peng et al., 2021b) to model equation 2. Orthogonal Random Fourier Features as well as trigonometric and hyperbolic approximations of softmax were used by (Choromanski

et al., 2020). Some authors follow the idea proposed by (Peng et al., 2021b) to project the input features to a number of dimensions larger than the number of input dimensions. Thereby, the low-rank constraint that other algorithms potentially suffer from can be mitigated or even eliminated.

4. Hadamard Linear Attention

4.1. Definition

Separable kernel functions are the basis of linear attention and enable compute and memory-efficient attention procedures. Since the nonlinearities are applied before the pairwise interactions are computed, linear attention models a low-rank approximation of pairwise interactions (Zhang et al., 2025). This is unlike *softmax*-based attention that applies the nonlinearity to the pairwise interactions.

The contribution made in this paper is to propose both a novel type of linear attention mechanism and a nonlinearity that is novel in linear attention. In contrast to existing works, this novel nonlinearity can be applied *after* the pairwise interactions have been computed. The proposed attention mechanism is therefore more similar to standard *softmax* attention. Although it would appear that such a model prohibits an efficient computational procedure to calculate attention, we will prove that our proposed attention mechanism allows for that, similar to linear attention.

Let $\phi_q : d \rightarrow d_\phi$ and $\phi_{k_f} : d \rightarrow d_\phi$ be nonlinear transformations with $f = 1, \dots, F$. We define our attention operator as follows

$$A = \left(\phi_q(Q) \cdot \phi_{k_1}(K)^\top \right) \odot \left(\phi_q(Q) \cdot \phi_{k_2}(K)^\top \right) \odot \dots \quad (5)$$

where the symbol \odot indicates the element-wise product, also called Hadamard product. Instead of *softmax* as nonlinearity, equation 5 uses the element-wise products $\prod_{f=1}^F \phi_q(q_i)^\top \cdot \phi_{k_f}(k_j)$. The attention update can be computed by right-multiplying A with the value matrix V . Please see the supplementary material for the definitions of networks ϕ_q and ϕ_{k_f} .

A major advantage of Hadamard Linear Attention over standard attention is that the low-rank constraint becomes less restrictive

$$\begin{aligned} \text{rank} \left(\left(\phi_q(Q) \cdot \phi_{k_1}(K)^\top \right) \odot \dots \odot \left(\phi_q(Q) \cdot \phi_{k_F}(K)^\top \right) \right) \\ \leq \prod_{f=1}^F \text{rank} \left(\phi_q(Q) \cdot \phi_{k_f}(K)^\top \right). \end{aligned} \quad (6)$$

Since the bottleneck imposed by the low-rank constraint is relaxed, a network based on HLA instead of standard linear attention achieves less information loss at each attention layer. This can lead to better performance.

4.2. Efficient Attention

Naïvely evaluating $A \cdot V$ by equation 5 has quadratic computational complexity. We now derive an efficient strategy for computing the attention, which will reveal a procedure analogous to that of standard linear attention. In the following, indicate by a summation symbol without any indices \sum a summation over all elements of the argument.

Lemma 4.1. *Given $F = 2$ factors for the Hadamard product in equation 5, we may express the product involving the d -dimensional vectors q , r^1 and r^2 as*

$$(q^\top \cdot r^1) \cdot (q^\top \cdot r^2) = \sum_{d \times d} \underbrace{(q \cdot q^\top)}_{d \times d} \odot \underbrace{(r^1 \cdot r^2^\top)}_{d \times d} \quad (7)$$

where the sum is over all the $\text{len}(q)^2$ elements.

For $F > 2$, the relation involving the d -dimensional vectors q and r^f generalizes to

$$\prod_{f=1}^F (q^\top \cdot r^f) = \sum_{d \times \dots \times d} \underbrace{(q \otimes \dots \otimes q)}_{d \times \dots \times d} \odot \underbrace{(r^1 \otimes \dots \otimes r^F)}_{d \times \dots \times d} \quad (8)$$

where the symbol \otimes denotes the outer tensorial product and the summation is over all the elements.

Proof. Given vectors a, b_1, \dots, b_n in \mathbb{R}^d , let $A = a \otimes a \otimes \dots \otimes a$ and $B = b_1 \otimes \dots \otimes b_n$. Let $[\mathcal{T}]_{i_1, \dots, i_n}$ be the operator that selects the entry at position i_1, \dots, i_n in tensor \mathcal{T} . Then, that element of tensor $\mathcal{A} \odot \mathcal{B}$ equals

$$\begin{aligned} [\mathcal{A} \odot \mathcal{B}]_{i_1, \dots, i_n} &= \mathcal{A}_{i_1, \dots, i_n} \cdot \mathcal{B}_{i_1, \dots, i_n} \\ &= (a_{i_1} \dots a_{i_n}) \cdot (b_1^{i_1} \dots b_n^{i_n}). \end{aligned} \quad (9)$$

Summing over all the entries of the tensor corresponding to the summation on the right hand side of equation 8, we may write

$$\begin{aligned} \sum_{i_1, \dots, i_n} a_{i_1} \dots a_{i_n} \cdot b_1^{i_1} \dots b_n^{i_n} \\ = \left(\sum_{i_1} a_{i_1} b_1^{i_1} \right) \dots \left(\sum_{i_n} a_{i_n} b_n^{i_n} \right) \\ = (a^\top b_1) \dots (a^\top b_n) \end{aligned} \quad (10)$$

which corresponds to the left hand side of equation 8 \square

Let \mathcal{T}_q be the $N \times d_\phi \times \dots \times d_\phi$ dimensional tensor that contains the N F -fold tensorial outer products of the vectors $\phi_q(q_i)$ with themselves, ie the i th slice, $i = 1, \dots, N$, is equivalent to $[\mathcal{T}_q]_i = \phi_q(q_i) \otimes \dots \otimes \phi_q(q_i)$. Analogously, define by \mathcal{T}_k the $N \times d_\phi \times \dots \times d_\phi$ tensor that contains the N F -fold tensorial outer products of the vectors $\phi_{k_f}(k_j)$.

Theorem 4.2. *The attention defined by equation 5 can be equivalently expressed by the product between \mathcal{T}_q and a $d_\phi \times \dots \times d_\phi \times d$ dimensional context tensor \mathcal{C} .*

Proof. Express the product between the j th column of the value matrix v_j and the i th row of the matrix of attention scores A_i by

$$\begin{aligned} A_i \cdot v_j &\stackrel{\text{L4.1}}{=} [\sum \mathcal{T}_{q_i} \odot \mathcal{T}_{k1} \quad \dots \quad \sum \mathcal{T}_{q_i} \odot \mathcal{T}_{kN}] \cdot v_j \\ &= \sum \mathcal{T}_{q_i} \odot \left(\sum_{i=1}^N v_{ij} \underbrace{(\phi_{k_1}(k_i) \otimes \dots \otimes \phi_{k_F}(k_i))}_{d_\phi \times \dots \times d_\phi} \right) \\ &= \sum \mathcal{T}_{q_i} \odot (\mathcal{T}_k \otimes_1 v_j). \end{aligned} \quad (11)$$

Recall that \otimes denotes the outer tensorial product between the $f = 1, \dots, F$ vectors $\phi_{k_f}(k_i)$. The symbol \otimes_1 means the contraction along the first dimension, ie multiplication and summation analogously to standard matrix-matrix multiplication. In other words, each of the $i = 1, \dots, N$ slices of size $d_\phi \times \dots \times d_\phi$ of tensor \mathcal{T}_k are multiplied by scalar v_{ij} . This result is element-wisely multiplied with \mathcal{T}_{q_i} and summed up.

For the complete matrix V , we compute the $d_\phi \times \dots \times d_\phi \times d$ dimensional tensor by

$$\mathcal{C} = \mathcal{T}_k \otimes_1 V. \quad (12)$$

Hence, the product $A \cdot V$ can be expressed by

$$A \cdot V = \mathcal{T}_q \otimes \mathcal{C}. \quad (13)$$

The contraction is over all dimensions of tensor \mathcal{T}_q except the first (the sequence) and all dimensions of tensor \mathcal{C} except the last one which corresponds to the number of columns of matrix V . \square

Please note that although equation 13 appears similar to the formulation of plain linear attention, it contains higher-order terms of the keys in \mathcal{C} via \mathcal{T}_k . In other words, linear attention computes attention scores linear in the keys, whereas HLA computes attention scores F -fold in the keys.

Lastly, we need to ensure that each row of matrix A sums up to 1. We may perform this similarly to standard linear attention if we require that $\phi_{q, k_1, k_2, k_3}(\cdot) \geq 0$. The factors η_i that normalize each row of the matrix in equation 5 to sum 1 are given by the contraction of the tensor $\mathcal{T}_q \odot \mathcal{T}_k$ over all dimensions except the first

$$\eta = \sum_{l, m, \dots} [\mathcal{T}_q \odot \mathcal{T}_k]_{l, m, \dots}. \quad (14)$$

A summary of the complete procedure is provided by algorithm 1 provided in the supplementary material. See Figs. 11 and 12 in the supplementary for PyTorch-like code of this algorithm.

4.3. Polynomial Degree and Complexity

Lemma 4.3. *The attention output $A \cdot V$, where the attention matrix A is defined by equation 5, is a rational function of the input variables. The numerator has degree $2^F + 1$, while the denominator has 2^F .*

Standard linear attention is equivalent to a rational function of degree 3 for the numerator and 2 for the denominator (Le tourneau et al., 2024). By equation 5, the claim follows.

This significantly larger degree enables the proposed algorithm to better perform the attention mechanism. The experimental results will show even a difference between $F = 2$ and $F = 3$ factors in the Hadamard product.

The computational complexity of the proposed algorithm is linear with respect to the sequence length. It grows polynomially with the number of factors in the Hadamard product in equation 5 $\mathcal{O}(d_\phi^F)$.

4.4. Causal Attention, Decay Factors and Sequential Updates

Since we require that $\phi_{q, k_1, k_2, k_3}(\cdot) \geq 0$ for normalization, we may easily consider, for instance, causal attention by left-multiplying an $n \times n$ matrix M to the keys $\phi_{k_f}(K)$. For causal attention, the entries of M are chosen to be $\{0, 1\}$. The mask can include decay factors as proposed in (Schlag et al., 2021).

Sequential Updates The proposed algorithm can be easily modified for efficient sequential updates. At the first token, tensor $\mathcal{T}_{k_1}^1 = \phi_{k_1}(k_1) \otimes \dots \otimes \phi_{k_F}(k_1)$ is multiplied d times with each of the d elements of $V = v_1^\top$

$$\mathcal{C}^1 = \mathcal{T}_{k_1} \boxtimes v_1, \quad (15)$$

where \boxtimes indicates the Kronecker product and $\mathcal{C}^1 \in \mathbb{R}^{d_\phi \times \dots \times d_\phi \times d}$. The query tensor at this point $\mathcal{T}_q^1 = \phi_q(q_1) \otimes \dots \otimes \phi_q(q_1)$ is element-wisely multiplied with each of the d slices of identical shape in \mathcal{C}^1 . Each of the d tensors is summed up to yield the d -dimensional results of the attention

$$\mathcal{O}^1 = \sum_{d_\phi^F} \mathcal{T}_q^1 \odot \mathcal{C}^1. \quad (16)$$

For any sequentially arriving new data at time $i > 1$, we only need to update the context tensor by adding

$$\mathcal{C}^i = \mathcal{C}^{i-1} + \mathcal{T}_{k_i} \boxtimes v_i, \quad (17)$$

and computing the product between \mathcal{T}_q^i and \mathcal{C}^i . In other words, the context tensor takes on the role of the state of the sequential attention.

Tensor \mathcal{T}_{k_i} has size d_ϕ^F , thus computing the product $\mathcal{T}_{k_i} \boxtimes v_i$ requires $d_\phi^F \cdot d$ floating point multiplications. Adding the

result to \mathcal{C}^{i-1} requires the same amount of floating point additions. If the hardware supports fused multiply-add, the total number of operations does not increase. Multiplying the context tensor to all the available queries in \mathcal{T}_q^i at time $N = i$ requires $N \cdot d_\phi^F \cdot d$ operations. Using a decay mechanism (Schlag et al., 2021; Yang et al., 2025a), this can be reduced to a total of only $3d_\phi^F d + N d d_\phi^F$ operations.

4.5. Value Modulation

Although Hadamard Linear Attention substantially mitigates the low-rank constraint that standard linear attention suffer from, we still observe degradation of high-frequency signal components.

To address this issue, we experimented with both a skip connection and a sigmoid-gated modulation. However, neither approach yielded satisfactory results.

It is important to note that gating by element-wise multiplication is equivalent to (circular) convolution in frequency domain. Since the sigmoid function maps inputs to the interval $[0, 1]$, it does not remove any frequency band, but it significantly attenuates them. Consequently, gating with a signal normalized by the sigmoid-function amounts to convolving with a kernel with tiny components, limiting the ability to recover high-frequency information.

To avoid the attenuation caused by sigmoid, we remove this activation and apply

$$T = T + \phi_{v_1}(T) \odot \phi_{v_2}(V) \quad (18)$$

where $T = A \cdot V$ indicates the result of the attention before applying the output mapping. Since the kernel corresponding to $\phi_{v_2}(V)$ has large support, the convolution can restore lost high-frequency information. See the supplementary for definitions of networks ϕ_{v_1} and ϕ_{v_2} .

5. Experiments

5.1. Implementation Details

Data We fine-tune our model variants using a 350K subset of the data used by OpenSoraPlan (Lin et al., 2024). We also use about 100K synthetic videos generated by Wan2.1 14B.

Model The proposed attention mechanism is integrated into the Wan2.1 1.3B model for video diffusion (et al., 2025). Two resolutions are used: first, the smaller of two resolutions used by the original model (81x480x832); second, a lower solution more suitable for fast video generation (81x320x480). The sequence lengths are 32760 and 12600 tokens, respectively. We indicate the two resolutions by **R1** and **R2**.

We evaluate with two variants of Hadamard Linear Attention. The first one employs three factors in equation 5, whereas

the second only uses two factors. For the first, we use small MLPs $\phi_q, \phi_{k_j}, j = \{1, 2, 3\}$ and $\phi_{v_l}, l = \{1, 2\}$. For the second, we use slightly larger MLPs.

The two HLA variants are included into four variants of Wan: **HLA-2F-R1-21** uses two factors in equation 5, a resolution of 81x480x832, and applies Hadamard Linear Attention to 21 out of 30 transformer blocks. **HLA-3F-R1-21** is identical to **HLA-2F-R1-21** except that it uses three factors in equation 5. **HLA-3F-R1-10** is identical to **HLA-3F-R1-21** except that it applies HLA to 10 transformer blocks. Lastly, **HLA-3F-R2-15** uses three factors for the Hadamard product in 15 out of 30 transformer blocks and resolution 81x320x480. Please see the supplementary material for more information about the model definitions.

Training Details We employ two training schemes. First, we only train the modified attention layers but keep all other layers fixed. This is followed by a second stage at which we train the entire transformer. We use the subset of (Lin et al., 2024) at these two stages. **HLA-2F-R1-21**, **HLA-3F-R1-10** and **HLA-3F-R2-15** are trained by this procedure. For **HLA-3F-R1-21**, we immediately train the entire transformer. At a third stage, we continue training the model but now include the synthetic data.

We use a learning rate of 1×10^{-4} for all models and all stages and use 8 H100 GPUs. The batch size is taken to be 16 for the last stage and 32 otherwise. For all but the first stages a warmup of 1000 steps is used. For all except the last stage, we use 100k training steps. At the last stage, we trained **HLA-2F-R1-21** for 50k steps, **HLA-3F-R1-10** for 90k steps, **HLA-3F-R2-15** for 110k steps and **HLA-3F-R1-21** for 140k steps.

Evaluation *VBench* (Huang et al., 2024) scores are reported to assess the visual quality and report the floating-point operations (FLOPs) of each model variant to measure the computational complexity. We evaluate against two checkpoints of Wan2.1 (et al., 2025), one at 480p provided by the original authors, the second at 320p trained by us. We do not compare with recent sophisticated variants of linear attention that use windowing, delta rule or hybrid methods that combine standard linear attention with softmax-attention. These techniques can be integrated into HLA, or HLA can replace standard linear attention in hybrid methods.

5.2. Main Results

We compare the performance of **HLA-3F-R1-10** with several state-of-the-art models of comparable number of parameters in table 1. For comparison, we used the *VBench* tool (Huang et al., 2024). High number indicate better results. As can be seen, the model using the proposed attention mechanism is slightly inferior. Compared with Wan2.1-1.3B, the model it is based on, it has about 23%

	Total↑	Quality↑	Semantic↑
Models with at most 2B parameters			
(Peng et al., 2025)	79.76	81.35	73.39
(Wu et al., 2025)	81.14	83.47	71.84
(HaCohen et al., 2024)	80.00	82.30	70.79
(Yang et al., 2025b)	81.55	82.48	77.81
(Isobe et al., 2025)	81.35	83.73	71.84
(Huang et al., 2025)	81.91	83.36	76.10
(Jin et al., 2025)	81.72	84.74	69.62
(Wan et al., 2025)	83.31	85.23	75.65
Wan2.1-1.3B-HLA			
~ 23% less total compute			
HLA-3F-R1-10	81.42	83.22	74.20

Table 1. Comparison on VBench with other models for video diffusion. We report the numbers published in the respective papers. While the proposed method has slightly lower scores, it requires less than 80% of the TFLOPs used by Wan2.1-1.3B.

lower computational complexity (cf. table 2).

5.3. Ablations

Table 2 shows a comparison of different model variants. They differ in whether they use two or three factors in the Hadamard product in equation 5 (indicated by **2F** or **3F**), the video resolution they were trained with (**R1** or **R2**) and the number of Hadamard Linear Attention Layers they use (**10**, **15** or **21**). It can be seen that the VBench scores slightly reduce while the number of HLA layers increases. Conversely, the computational complexity reduces. The time necessary to generate a single video is perceivably lower for **HLA-3F-R1-21** compared to the baseline. **HLA-3F-R1-21** requires almost half the number of floating-point operations (FLOPs) as the baseline. We also see that 3-factor HLA provides better performance than 2-factor, despite that the 2-factor version has similar FLOPs (by using larger MLPs). The reason that the computation time does not reduce as much as the number of FLOPs lies in the number of compute units that allow massive parallelization. Less capable accelerators, for instance those widely used in mobile applications, can be expected to benefit even more from the proposed algorithm. This shows that using higher-degree HLA is a more effective way to scale up model capacity.

5.4. Complexity

Table 3 compares the computational complexities of the four different HLA variants compared with standard quadratic attention. As in Sec. 5.1, we use slightly larger MLPs for HLA with 2 factors. Depending on the resolution and the algorithmic variant, HLA requires between 20% and 90% less floating-point operations (FLOPs) than quadratic attention. Fig. 7 shows a comparison of the necessary FLOPs of

2-factor and 3-factor HLA with standard attention across a range of sequence lengths.

Method	Tokens	Score	TFLOPs	Time
Wan2.1 (quad.)	32760	83.3	283.03	1:36
Wan2.1 (quad.)	12600	81.0	62.13	0:45
HLA-3F-R1-10	32760	81.42	218.59	1:26
HLA-3F-R2-15	12600	79.78	48.37	0:26
HLA-2F-R1-21	32760	79.02	147.16	1:13
HLA-3F-R1-21	32760	80.54	147.71	1:16

Table 2. VBench scores and times to generate a single video of several model variants. TFLOPs are for a single forward pass through the model. All measurement were done on an H100 GPU.

Attn Type	Resolution	Tokens	TFLOPs
Wan2.1 (quad.)	320x480	12600	1.21
Wan2.1 (quad.)	480x832	32760	7.21
HLA 2 factors	320x480	12600	0.97
HLA 2 factors	480x832	32760	2.52
HLA 3 factors	320x480	12600	0.30
HLA 3 factors	480x832	32760	0.77

Table 3. Computational complexity of models with 2 or 3 factors in the Hadamard product in equation 5 for 12600 or 32760 tokens.

5.5. Qualitative Examples

Qualitative examples of videos generated with the proposed attention mechanism are shown in Figs 1 and 2. These results demonstrate the higher nonlinearity of HLA indeed suffices to bridge the performance gap that separates standard linear attention from quadratic softmax attention. See the supplementary for more examples and videos.

6. Conclusions

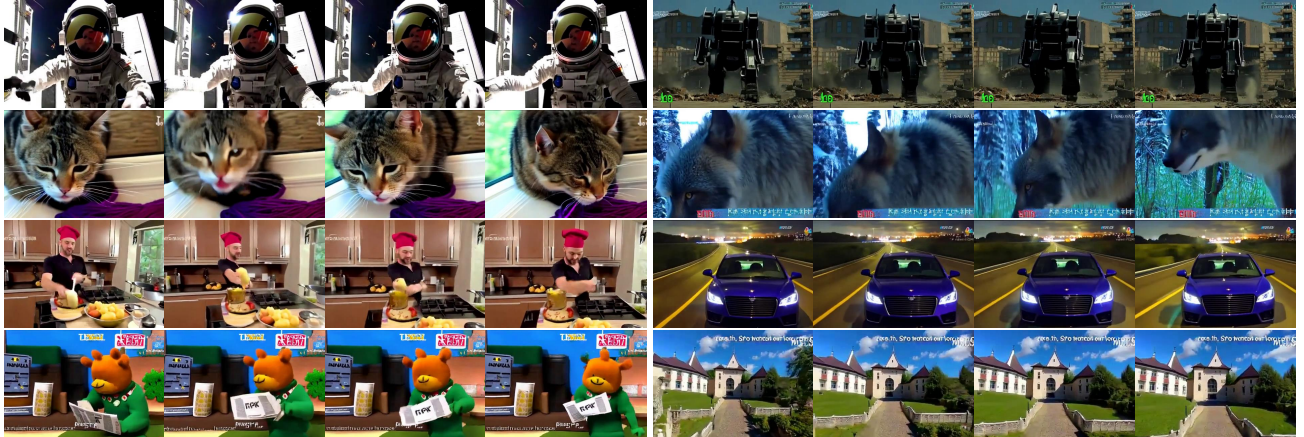
We proposed Hadamard Linear Attention (HLA), a novel algorithm to compute attention. Unlike traditional linear attention algorithms, HLA applies a nonlinearity after the pairwise similarities have been computed. We derived an efficient formulation that reduces the complexity to $\mathcal{O}(N)$. HLA relies on standard tensor operations and can directly operate on the input sequence without requiring any time-consuming tensor reshaping. We demonstrated good results on the challenging application of video diffusion which involves extremely long sequences. For typical sequence lengths, our proposed HLA requires only about 1/10 of the FLOPs that baselines need. HLA can replace standard linear attention in hybrid algorithms like (Zhang et al., 2025) and (Ghafoorian et al., 2025) to yield improved performance. Likewise, HLA can be extended with windowing or the delta-rule to improve the algorithm.



(a) Results HLA-3F-R1-10



(b) Results HLA-3F-R1-21



(c) Results HLA-3F-R2-15

Figure 2. Examples of generated videos by **HLA-3F-R1-10** (upper videos) and **HLA-3F-R1-21** (lower videos). It can be seen that the methods using the proposed attention mechanism indeed generate high-quality videos. Please see the supplementary material for more examples.

References

Chen, J., Zhao, Y., Yu, J., Chu, R., Chen, J., Yang, S., Wang, X., Pan, Y., Zhou, D., Ling, H., Liu, H., Yi, H., Zhang, H., Li, M., Chen, Y., Cai, H., Fidler, S., Luo, P., Han, S., and Xie, E. Sana-video: Efficient video generation with block linear diffusion transformer, 2025. URL <https://arxiv.org/abs/2509.24695>.

Choromanski, K., Likhosherstov, V., Dohan, D., Song, X., Gane, A., Sarlos, T., Hawkins, P., Davis, J., Mohiuddin, A., Kaiser, L., Belanger, D., Colwell, L., and Weller, A. Rethinking attention with performers. *arXiv preprint arXiv:2009.14794*, 2020. URL <https://arxiv.org/abs/2009.14794>.

Choromanski, K., Likhosherstov, V., Dohan, D., Song, X., Gane, A., Sarlos, T., Hawkins, P., Davis, J., Mohiuddin, A., Kaiser, L., Belanger, D., Colwell, L., and Weller, A. Rethinking attention with performers, 2022. URL <https://arxiv.org/abs/2009.14794>.

Dao, T. Flashattention-2: Faster attention with better parallelism and work partitioning. *arXiv preprint arXiv:2307.08691*, 2023. URL <https://arxiv.org/abs/2307.08691>.

Dao, T. and Gu, A. Transformers are ssms: Generalized models and efficient algorithms through structured state space duality, 2024. URL <https://arxiv.org/abs/2405.21060>.

Dao, T., Fu, D. Y., Ermon, S., Rudra, A., and Ré, C. Flashattention: Fast and memory-efficient exact attention with io-awareness. *Advances in Neural Information Processing Systems*, 35:16344–16359, 2022.

Egorov, E., Ackermann, H., Nagel, M., and Cai, H. Myosotis: structured computation for attention like layer, 2025. URL <https://arxiv.org/abs/2509.20503>.

et al., T. W. Open and advanced large-scale video generative models, 2025. URL <https://arxiv.org/abs/2503.20314>.

Fan, Q., Huang, H., and He, R. Breaking the low-rank dilemma of linear attention, 2025a. URL <https://arxiv.org/abs/2411.07635>.

Fan, Q., Huang, H., and He, R. Breaking the low-rank dilemma of linear attention, 2025b.

Ghafoorian, M., Korzhenkov, D., and Habibian, A. Attention surgery: An efficient recipe to linearize your video diffusion transformer, 2025. URL <https://arxiv.org/abs/2509.24899>.

Gu, A. and Dao, T. Mamba: Linear-time sequence modeling with selective state spaces, 2024. URL <https://arxiv.org/abs/2312.00752>.

Gu, A., Goel, K., and Ré, C. Efficiently modeling long sequences with structured state spaces, 2022.

HaCohen, Y., Chiprut, N., Brazowski, B., Shalem, D., Moshe, D., Richardson, E., Levin, E., Shiran, G., Zabari, N., Gordon, O., Panet, P., Weissbuch, S., Kulikov, V., Bitterman, Y., Melumian, Z., and Bibi, O. Ltx-video: Realtime video latent diffusion, 2024. URL <https://arxiv.org/abs/2501.00103>.

Han, I., Jayaram, R., Karbasi, A., Mirrokni, V., Woodruff, D. P., and Zandieh, A. Hyperattention: Long-context attention in near-linear time, 2023. URL <https://arxiv.org/abs/2310.05869>.

Huang, J., Zhang, G., Jie, Z., Jiao, S., Qian, Y., Chen, L., Wei, Y., and Ma, L. M4v: Multi-modal mamba for text-to-video generation, 2025. URL <https://arxiv.org/abs/2506.10915>.

Huang, Z., He, Y., Yu, J., Zhang, F., Si, C., Jiang, Y., Zhang, Y., Wu, T., Jin, Q., Chanpaisit, N., Wang, Y., Chen, X., Wang, L., Lin, D., Qiao, Y., and Liu, Z. Vbench: Comprehensive benchmark suite for video generative models. In *Computer Vision and Pattern Recognition (CVPR)*, 2024.

Isobe, T., Cui, H., Zhou, D., Ge, M., Li, D., and Barssoum, E. Amd-hummingbird: Towards an efficient text-to-video model, 2025. URL <https://arxiv.org/abs/2503.18559>.

Jin, Y., Sun, Z., Li, N., Xu, K., Xu, K., Jiang, H., Zhuang, N., Huang, Q., Song, Y., Mu, Y., and Lin, Z. Pyramidal flow matching for efficient video generative modeling, 2025. URL <https://arxiv.org/abs/2410.05954>.

Katharopoulos, A., Vyas, A., Pappas, N., and Fleuret, F. Transformers are RNNs: Fast autoregressive transformers with linear attention. In *Proceedings of the 37th International Conference on Machine Learning (ICML)*, pp. 5156–5165, 2020.

Letourneau, P.-D., Singh, M. K., Cheng, H.-P., Han, S., Shi, Y., Jones, D., Langston, M. H., Cai, H., and Porikli, F. Padre: A unifying polynomial attention drop-in replacement for efficient vision transformer, 2024. URL <https://arxiv.org/abs/2407.11306>.

Lin, B., Ge, Y., Cheng, X., Li, Z., Zhu, B., Wang, S., He, X., Ye, Y., Yuan, S., Chen, L., Jia, T., Zhang, J., Tang, Z., Pang, Y., She, B., Yan, C., Hu, Z., Dong, X., Chen, L., Pan, Z., Zhou, X., Dong, S., Tian, Y., and Yuan, L. Open-sora plan: Open-source large video generation model, 2024. URL <https://arxiv.org/abs/2412.00131>.

Meng, W., Luo, Y., Li, X., Jiang, D., and Zhang, Z. Polarformer: Polarity-aware linear attention for vision transformers. In *International Conference on Learning Representations (ICLR)*, 2025. URL <https://openreview.net/forum?id=kN6MFmKUSK>.

Peng, H., Pappas, N., Yogatama, D., Schwartz, R., Smith, N. A., and Kong, L. Random feature attention. In *International Conference on Learning Representations (ICLR)*, 2021a.

Peng, H., Pappas, N., Yogatama, D., Schwartz, R., Smith, N. A., and Kong, L. Random feature attention. *CoRR*, abs/2103.02143, 2021b. URL <https://arxiv.org/abs/2103.02143>.

Peng, X., Zheng, Z., Shen, C., Young, T., Guo, X., Wang, B., Xu, H., Liu, H., Jiang, M., Li, W., Wang, Y., Ye, A., Ren, G., Ma, Q., Liang, W., Lian, X., Wu, X., Zhong, Y., Li, Z., Gong, C., Lei, G., Cheng, L., Zhang, L., Li, M., Zhang, R., Hu, S., Huang, S., Wang, X., Zhao, Y., Wang, Y., Wei, Z., and You, Y. Open-sora 2.0: Training a commercial-level video generation model in \$200k, 2025. URL <https://arxiv.org/abs/2503.09642>.

Qin, Z., Sun, W., Deng, H., Li, D., Wei, Y., Lv, B., Yan, J., Kong, L., and Zhong, Y. cosformer: Rethinking softmax in attention. In *International Conference on Learning Representations (ICLR)*, 2022.

Qiu, Z., Wang, Z., Zheng, B., Huang, Z., Wen, K., Yang, S., Men, R., Yu, L., Huang, F., Huang, S., Liu, D., Zhou, J., and Lin, J. Gated attention for large language models: Non-linearity, sparsity, and attention-sink-free, 2025. URL <https://arxiv.org/abs/2505.06708>.

Schlag, I., Irie, K., and Schmidhuber, J. Linear transformers are secretly fast weight programmers. In *Proceedings of the 37th International Conference on Machine Learning*, Proceedings of Machine Learning Research. PMLR, 2021.

Schmidhuber, J. Learning to control fast-weight memories: An alternative to dynamic recurrent networks. *Neural Computation*, 4(1):131–139, 1992. doi: 10.1162/neco.1992.4.1.131.

Shah, J., Bikshandi, G., Zhang, Y., Thakkar, V., Ramani, P., and Dao, T. Flashattention-3: Fast and accurate attention with asynchrony and low-precision, 2024. URL <https://arxiv.org/abs/2407.08608>.

Shen, Z., Zhang, M., Zhao, H., Yi, S., and Li, H. Efficient attention: Attention with linear complexities. In *Winter Conference on Applications of Computer Vision (WACV)*, 2024.

Sima, C., Renz, K., Chitta, K., Chen, L., Zhang, H., Xie, C., Beißwenger, J., Luo, P., Geiger, A., and Li, H. Drivelm: Driving with graph visual question answering. In *European Conference on Computer Vision (ECCV)*, 2024.

Sun, Y., Dong, L., Huang, S., Ma, S., Xia, Y., Xue, J., Wang, J., and Wei, F. Retentive network: A successor to transformer for large language models, 2023. URL <https://arxiv.org/abs/2307.08621>.

Team, K., Zhang, Y., Lin, Z., Yao, X., Hu, J., Meng, F., Liu, C., Men, X., Yang, S., Li, Z., Li, W., Lu, E., Liu, W., Chen, Y., Xu, W., Yu, L., Wang, Y., Fan, Y., Zhong, L., Yuan, E., Zhang, D., Zhang, Y., Liu, T. Y., Wang, H., Fang, S., He, W., Liu, S., Li, Y., Su, J., Qiu, J., Pang, B., Yan, J., Jiang, Z., Huang, W., Yin, B., You, J., Wei, C., Wang, Z., Hong, C., Chen, Y., Chen, G., Wang, Y., Zheng, H., Wang, F., Liu, Y., Dong, M., Zhang, Z., Pan, S., Wu, W., Wu, Y., Guan, L., Tao, J., Fu, G., Xu, X., Wang, Y., Lai, G., Wu, Y., Zhou, X., Yang, Z., and Du, Y. Kimi linear: An expressive, efficient attention architecture, 2025. URL <https://arxiv.org/abs/2510.26692>.

Vaswani, A., Shazeer, N., Parmar, N., Uszkoreit, J., Jones, L., Gomez, A. N., Kaiser, L., and Polosukhin, I. Attention is all you need. In *Advances in Neural Information Processing Systems*, pp. 5998–6008, 2017.

Wan, T., Wang, A., Ai, B., Wen, B., Mao, C., Xie, C.-W., Chen, D., Yu, F., Zhao, H., Yang, J., Zeng, J., Wang, J., Zhang, J., Zhou, J., Wang, J., Chen, J., Zhu, K., Zhao, K., Yan, K., Huang, L., Feng, M., Zhang, N., Li, P., Wu, P., Chu, R., Feng, R., Zhang, S., Sun, S., Fang, T., Wang, T., Gui, T., Weng, T., Shen, T., Lin, W., Wang, W., Wang, W., Zhou, W., Wang, W., Shen, W., Yu, W., Shi, X., Huang, X., Xu, X., Kou, Y., Lv, Y., Li, Y., Liu, Y., Wang, Y., Zhang, Y., Huang, Y., Li, Y., Wu, Y., Liu, Y., Pan, Y., Zheng, Y., Hong, Y., Shi, Y., Feng, Y., Jiang, Z., Han, Z., Wu, Z.-F., and Liu, Z. Wan: Open and advanced large-scale video generative models, 2025. URL <https://arxiv.org/abs/2503.20314>.

Wang, S., Leroy, V., Cabon, Y., Chidlovskii, B., and Revaud, J. Dust3r: Geometric 3d vision made easy, 2024. URL <https://arxiv.org/abs/2312.14132>.

Wei, J., Wang, X., Schuurmans, D., Bosma, M., Ichter, B., Xia, F., Chi, E. H., Le, Q. V., and Zhou, D. Chain-of-thought prompting elicits reasoning in large language models. In *Advances in Neural Information Processing Systems (NeurIPS)*, 2022. URL https://openreview.net/forum?id=_VjQ1MeSB_J.

Wu, Y., Zhang, Z., Li, Y., Xu, Y., Kag, A., Sui, Y., Coskun, H., Ma, K., Lebedev, A., Hu, J., Metaxas, D., Wang, Y., Tulyakov, S., and Ren, J. Snagen-v: Generating

a five-second video within five seconds on a mobile device, 2025. URL <https://arxiv.org/abs/2412.10494>.

Wu, Z., Ding, T., Lu, Y., Pai, D., Zhang, J., Wang, W., Yu, Y., Ma, Y., and Haeffele, B. D. Token statistics transformer: Linear-time attention via variational rate reduction, 2024. URL <https://arxiv.org/abs/2412.17810>.

Xie, E., Chen, J., Chen, J., Cai, H., Tang, H., Lin, Y., Zhang, Z., Li, M., Zhu, L., Lu, Y., and Han, S. Sana: Efficient high-resolution image synthesis with linear diffusion transformers, 2024. URL <https://arxiv.org/abs/2410.10629>.

Yang, S., Kautz, J., and Hatamizadeh, A. Gated delta networks: Improving mamba2 with delta rule, 2025a. URL <https://arxiv.org/abs/2412.06464>.

Yang, Z., Teng, J., Zheng, W., Ding, M., Huang, S., Xu, J., Yang, Y., Hong, W., Zhang, X., Feng, G., Yin, D., Zhang, Y., Wang, W., Cheng, Y., Xu, B., Gu, X., Dong, Y., and Tang, J. Cogvideox: Text-to-video diffusion models with an expert transformer, 2025b. URL <https://arxiv.org/abs/2408.06072>.

Ye, T., Dong, L., Xia, Y., Sun, Y., Zhu, Y., Huang, G., and Wei, F. Differential transformer, 2025. URL <https://arxiv.org/abs/2410.05258>.

Zhang, J., Wang, H., Jiang, K., Yang, S., Zheng, K., Xi, H., Wang, Z., Zhu, H., Zhao, M., Stoica, I., Gonzalez, J. E., Zhu, J., and Chen, J. Sla: Beyond sparsity in diffusion transformers via fine-tunable sparse-linear attention, 2025. URL <https://arxiv.org/abs/2509.24006>.

Zhu, L., Huang, Z., Liao, B., Liew, J. H., Yan, H., Feng, J., and Wang, X. Dig: Scalable and efficient diffusion models with gated linear attention, 2024. URL <https://arxiv.org/abs/2405.18428>.

A. Model Definitions

A.1. Defining ϕ

We use models with few parameters for the networks ϕ_q , $\phi_{k_{1,2,3}}$ and $\phi_{v_{1,2}}$ (see Fig. 3). They consist of two linear layers with a GELU activation in between and an optional RELU activation for ϕ_q and $\phi_{k_{1,2,3}}$. We experienced instabilities during training if $\phi_{v_{1,2}}$ did not use a LayerNorm.

For the first linear layer, we used the head dimension ($1536/12 = 128$) as input and output. For $\phi_{v_{1,2}}$, we used the same number of inputs and outputs for the second linear layer. Otherwise, we use 6 output channels if 3-factor HLA, or 12 channels if 2-factor HLA.

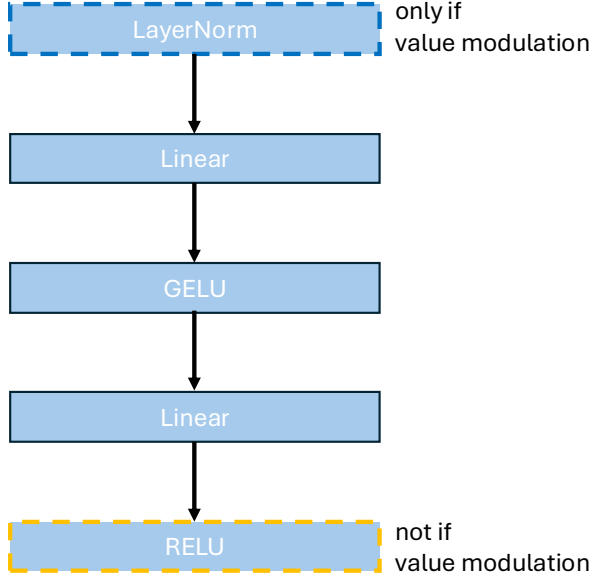


Figure 3. Definition of networks $\phi_{q,k_{1,2,3},v}$

For ϕ_{v_1} , we first tried to use a sigmoid activation, yet that had no effect.

A.2. Model Variants

We computed maximal attention scores for each self-attention block of the teacher model averaged over several batches. For **HLA-3F-R1-21**, we selected the 21 blocks (1,2,3,4,5,6,7,8, 11,12,13,14,15,16,17,18, 22,23,24,25,26) with the smallest scores. For **HLA-3F-R2-15**, we did not use HLA in the last 6 blocks that (1,2,3,4,5,6,7,8, 11,12,13,14,15,16,17). For **HLA-3F-R1-10**, we only use HLA in the odd layers (1,3,5,7, 11,13,15,17, 23,25).

A.3. Pseudocode

Algorithm 1 provides pseudocode of the entire attention procedure. PyTorch-like code for the implementation of the subroutines to compute two or three factor HLA can be found in figures 11 and 12.

B. Value Modulation

To demonstrate the positive effect that our proposed value modulation module has, we generated a video using **HLA-3F-R1-21** and 50 sampling steps. The first image of the generated sequence is shown in Fig. 5.

Table 4 shows attention updates *before* value modulation at different sampling steps (columns) and different transformer blocks (rows). We reshape the tensor to undo splitting into several heads. The 1536 channels are projected onto 3

Algorithm 1 Hadamard Linear Attention**Input:** Input tokens X **Output:** Attention output**Step 1: Generate queries, keys, values** $q, k, v \leftarrow \text{to_q}(X), \text{to_k}(X), \text{to_v}(X)$

reshape tensors to allow for multi-head attention

Step 2: Apply rotational embedding $q, k \leftarrow \text{apply_rope}(q), \text{apply_rope}(k)$ **Step 3: Apply scale factor** $q \leftarrow q \cdot \text{scale_factor}$ **Step 4: HLA-specific transformations** $q \leftarrow \text{hla_to_q}(q)$ $k_1, k_2 \leftarrow \text{hla_to_k1}(k), \text{hla_to_k2}(k)$ **if** use_hla_3_factors **then** $k_3 \leftarrow \text{hla_to_k3}(k)$ **end if****Step 5: Compute HLA****if** use_hla_2_factors **then**

by algorithm in Fig. 4 (supplementary)

 $\text{attn} \leftarrow \text{2_factor_hla}(q, k_1, k_2, v)$ **end if****if** use_hla_3_factors **then**

by algorithm in Fig. 5 (supplementary)

 $\text{attn} \leftarrow \text{3_factor_hla}(q, k_1, k_2, k_3, v)$ **end if****Return** $\text{to_out}(\text{attn})$

channels by a random projection matrix whose entries are chosen from a uniform distribution $\in [0, 1]$. Afterwards, we normalize the tensor, so that all entries are in $[0, 1]$. We can see that the self attention in the middle transformer blocks 11 and 18 contribute much to the overall structure.

Table 5 shows the contributions of the value modulation. We can see that this module adds to the structure at steps 30, 40 and 40 at blocks 2 and 3, already. Blocks 4 and 11 apparently add significant structure mainly at steps 10, 20, 30 and 40. Block 26 adds high-frequency information at all higher sampling steps.

C. VBench Scores

We provide VBench scores per category in Fig. 4. The dark blue line corresponds to **HLA-3F-R1-10**, the light blue line to **HLA-3F-R1-21** and the red line to **HLA-3F-R2-15**.

VBench scores at different training iterations of the last stage that includes the synthetic data can be seen in Fig. 6. The colors indicate the same variants as in Fig. 4. The increase observable for all three methods demonstrates the positive impact our synthetic data has.

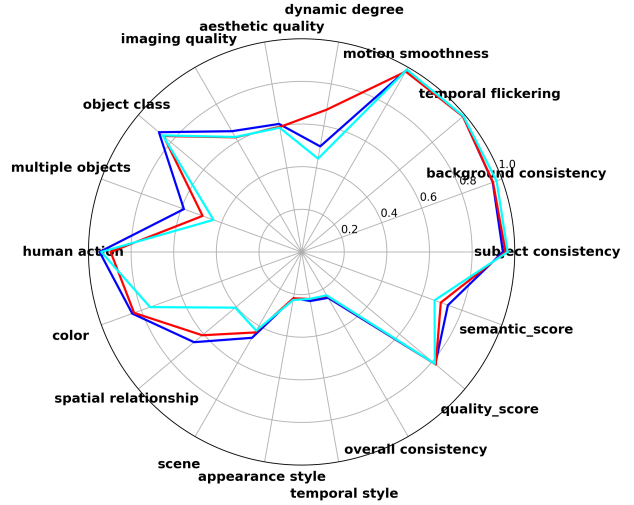


Figure 4. VBench scores by categories. Dark blue line corresponds to **HLA-3F-R1-10**, red to **HLA-3F-R1-21** and light blue to **HLA-3F-R2-15**.



Figure 5. First image of a video generated by **HLA-3F-R1-21** in 50 steps.

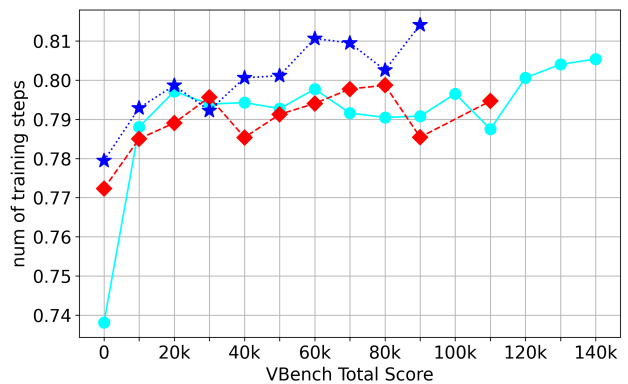


Figure 6. VBench scores over iterations. VBench scores are computed using 40% of prompts. The blue line indicates **HLA-3F-R1-10**, the red line **HLA-3F-R2-15** and the light blue line **HLA-3F-R1-21**.

Table 4. Attention output before value modulation. Columns correspond to different sampling steps in the generation process. Rows indicate the index of the transformer block.

	Step 1	Step 10	Step 20	Step 30	Step 40	Step 50
1						
2						
3						
4						
11						
18						
26						

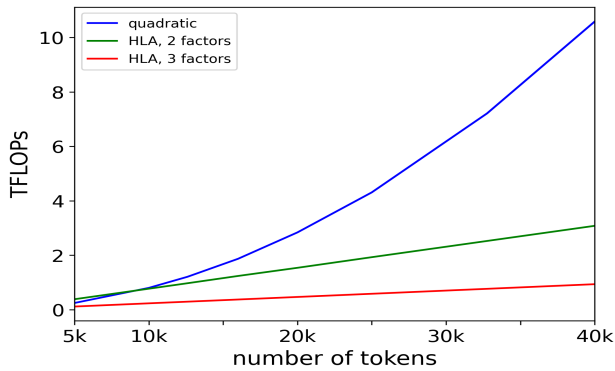


Figure 7. Comparison of computational complexities for different sequence lengths between standard quadratic attention and 2 or 3-factor HLA.

Table 5. Contributions to attention update by value modulation. Columns correspond to different sampling steps in the generation process. Rows indicate the index of the transformer block.

	Step 1	Step 10	Step 20	Step 30	Step 40	Step 50
1						
2						
3						
4						
11						
18						
26						

D. Qualitative Examples

We present further qualitative examples of all three variants in Figs. 8, 9 and 10. As can be seen, all three methods achieve to generate high-quality videos. Please also see the original mp4 files in the supplementary material.

E. Code Listings

We provide PyTorch-like code in listings 11 and 12. These algorithms do not require time-consuming tensor reshaping. They only require elementary computational operations.

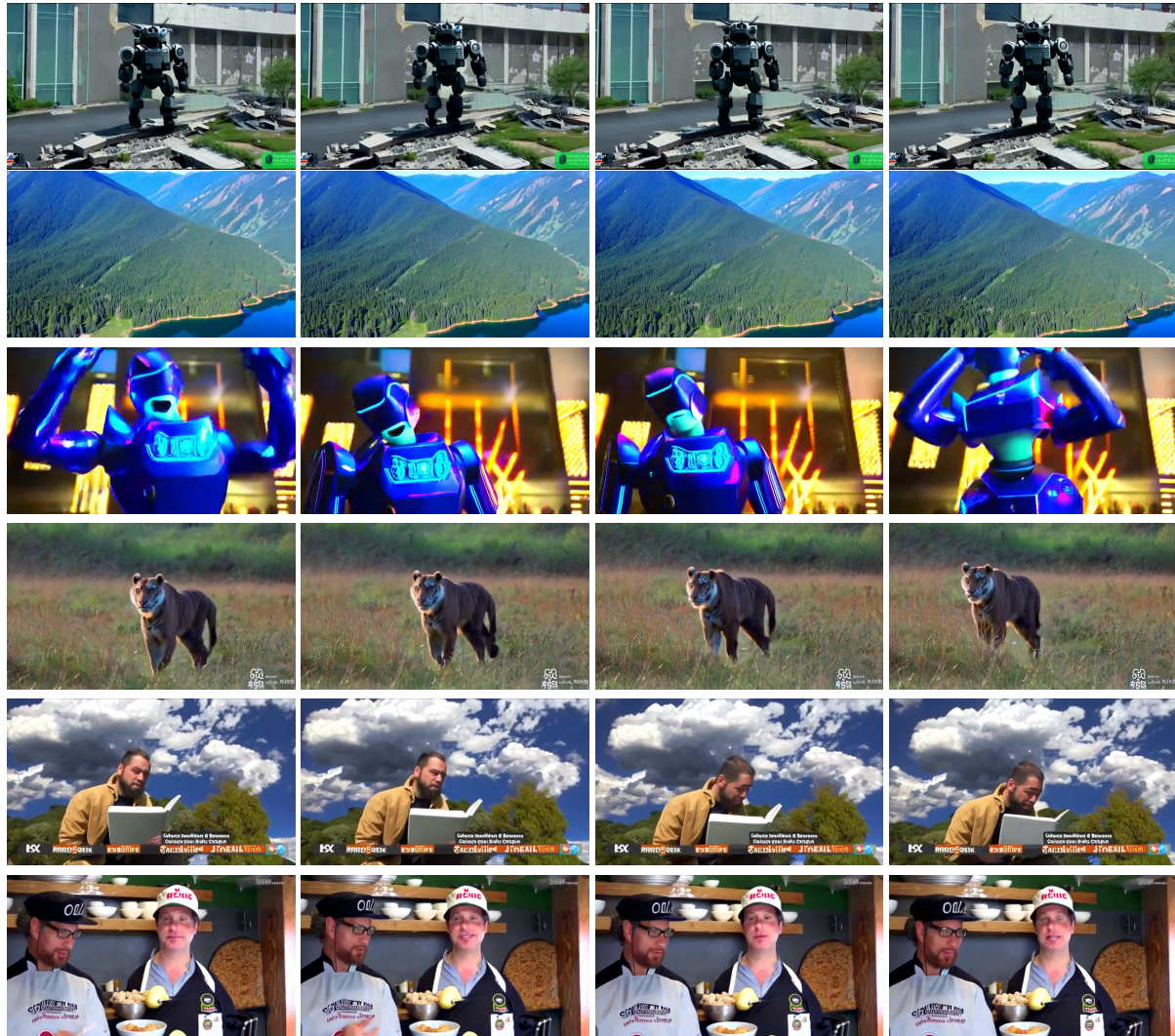


Figure 8. Qualitative Examples **HLA-3F-R1-10**



Figure 9. Qualitative Examples **HLA-3F-R1-21**

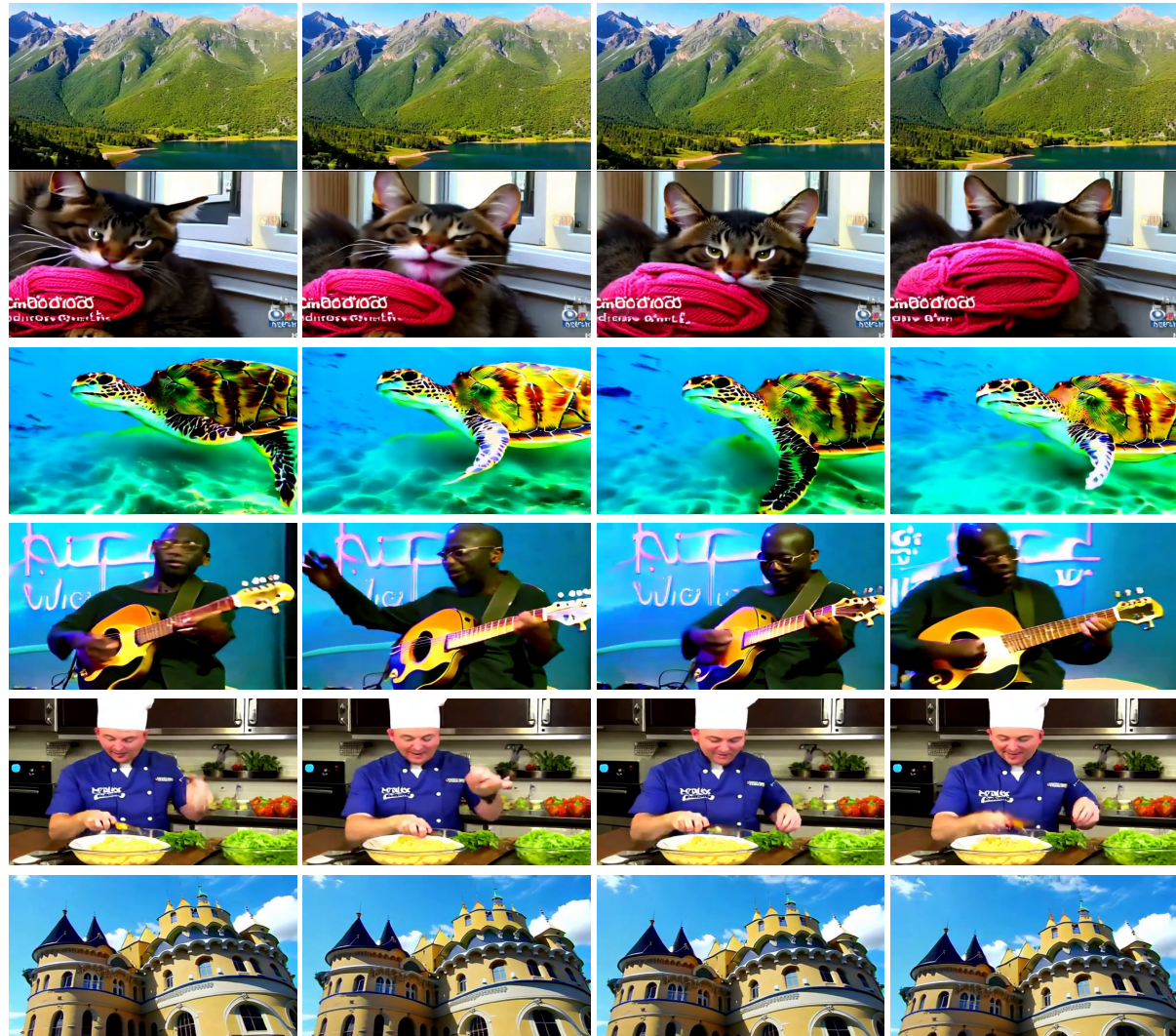


Figure 10. Qualitative Examples **HLA-3F-R2-15**

```

1 def HLA_2_factors(query, key1, key2, value):
2     # equivalent to ((Q@K1.t()) * (Q@K2.t())) @ V
3     # (omitting normalization for simplicity)
4
5     # batch size, number of heads, sequence length, d_phi
6     bs, nh, sl, dp = query.shape
7     d = value.shape[-1]
8
9     # compute outer products between query and key1, key2 tokens
10    k_outerprod_k = torch.einsum('bhsd,bhse->bhsde',key1, key2)
11    context = torch.einsum(
12        'bhmde,bhmg->bhdeg',
13        k_outerprod_k, value
14    )
15    q_outerprod_q = torch.einsum('bhsd,bhse->bhsde',query, query)
16
17    # normalization
18    sum_over_k = k_outerprod_k.sum(dim=2, keepdim=True)
19    eta = torch.sum(
20        q_outerprod_q.view(bs, nh, sl, -1)
21        *
22        sum_over_k.view(bs, nh, 1, -1),
23        dim=-1, keepdim=True
24    )
25    q_outerprod_q = q_outerprod_q / (eta.view(bs, nh, sl, 1, 1)+eps)
26
27    # memory efficient computation
28    q_outerprod_q = q_outerprod_q.view(bs, nh, sl, dp**2)
29    context = context.view(bs, nh, dp**2, d)
30
31    # output of linear attention (before ouput projection)
32    attention = torch.einsum(
33        'bhsd,bhde->bhse',
34        q_outerprod_q, context
35    )
36
37    return attention

```

Figure 11. PyTorch-like code of Hadamard Linear Attention with 2 factors.

```

1 def HLA_3_factors(query, key1, key2, key3, value):
2     # equivalent to ((Q@K1.t()) * (Q@K2.t()) * (Q@K3.t())) @ V
3     # (omitting normalization for simplicity)
4
5     # batch size, number of heads, sequence length, d_phi
6     bs, nh, sl, dp = query.shape
7     d = value.shape[-1]
8
9     # compute outer products between query and key1, key2 tokens
10    k_outerprods = torch.einsum(
11        'bhsd,bhse,bhsf->bhsdef',
12        key1, key2, key3
13    )
14    context = torch.einsum(
15        'bhmdef,bhmg->bhdefg',
16        k_outerprods, value
17    )
18    q_outerprods = torch.einsum(
19        'bhsd,bhse,bhsf->bhsdef',
20        query, query, query
21    )
22
23     # normalization
24    sum_over_k = k_outerprods.sum(dim=2, keepdim=True)
25    eta = torch.sum(
26        q_outerprods.view(bs, nh, sl, -1)
27        *
28        sum_over_k.view(bs, nh, 1, -1),
29        dim=-1, keepdim=True
30    )
31    q_outerprods = q_outerprods / (eta.view(bs, nh, sl, 1, 1, 1)+eps)
32
33     # memory efficient computation
34    q_outerprods = q_outerprods.view(bs, nh, sl, dp**3)
35    context = context.view(bs, nh, dp**3, d)
36
37     # output of linear attention (before ouput projection)
38    attention = torch.einsum(
39        'bhsd,bhde->bhse',
40        q_outerprods, context
41    )
42
43    return attention

```

Figure 12. PyTorch-like code of Hadamard Linear Attention with 3 factors.